

Reaction Mechanisms

Experimental and Computational Studies on the C–H Amination Mechanism of Tetrahydrocarbazoles via Hydroperoxides

Naeem Gulzar,^[a] Kevin Mark Jones,^[a] Hannelore Konnerth,^[b] Martin Breugst,^{*[b]} and Martin Klussmann^{*[a]}

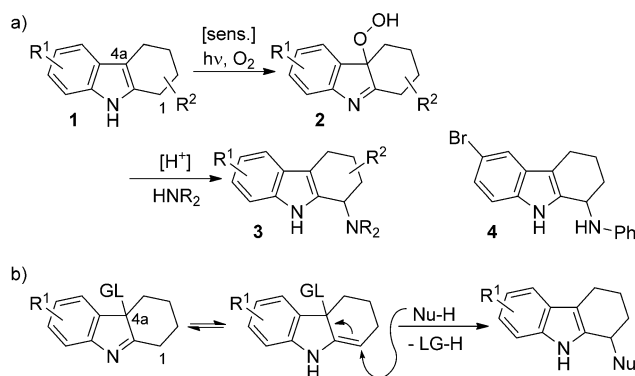
Abstract: The acid-catalyzed reactions of photochemically generated tetrahydrocarbazole peroxides with anilines have been studied experimentally and computationally to identify the underlying reaction mechanism. The kinetic data indicate a reaction order of one in the hydroperoxide and zero in the aniline. Computational investigations using density functional theory support the experimental findings and pre-

dict an initial tautomerization between an imine and enamine substructure of the primarily generated tetrahydrocarbazole peroxide to be the rate controlling step. The enamine tautomer then loses hydrogen peroxide upon protonation, generating a stabilized allylic carbocation that is reversibly trapped by solvent or aniline to form the isolated products.

Introduction

Oxidative coupling reactions for the functionalization of C–H bonds have emerged as an important synthetic tool in recent years.^[1] They help to save time, steps, and materials as two substrates can be directly coupled without the need for pre-functionalization. However, some of these reactions require harsh conditions and their overall sustainability is further diminished if stoichiometric amounts of synthetic oxidants are required. This problem can be overcome by using catalytic conditions and environmentally benign molecular oxygen as the terminal oxidant.^[1a,2]

We recently reported a Brønsted-acid-catalyzed aerobic amination of tetrahydrocarbazole and indole derivatives by using the strategy of C–H functionalization via Intermediate PeroxideS (CHIPS, Scheme 1a).^[3] By treating the starting materials, for example, tetrahydrocarbazoles **1**, with oxygen in the presence of visible light and a photosensitizer, hydroperoxides **2** are generated. These can be subjected to acid catalysis in the presence of anilines and some other N-nucleophiles, giving the substitution products **3**. The hydroperoxides can be conveniently isolated prior to substitution, but they can also be directly subjected to the second step in a one-pot procedure. The reactions do not require elevated temperatures, stoichiometric



Scheme 1. a) Amination of tetrahydrocarbazole derivatives **1** by the strategy of C–H functionalization via intermediate peroxides (CHIPS); b) common proposal for the observed shift from the 4a to the 1 position during nucleophilic substitution reactions with activated tetrahydrocarbazoles.

amounts of synthetic oxidants, or expensive metal catalysts, but simply visible light, a sensitizer, and a simple Brønsted acid. The latter can either be trifluoroacetic acid in catalytic amounts or acetic acid as solvent, depending on the nature of the substrates.^[3a] The reaction could be applied to the synthesis of pharmaceutically active compounds such as **4** (Scheme 1), which has antiviral properties in the nanomolar range.^[4]

The interesting shift occurring in the transformation of **2** to **3**, which substitutes the hydroperoxide at position 4a to install the N-nucleophile at position 1 (Scheme 1a), has been observed in a couple of related cases before. Substitution reactions with tetrahydrocarbazoles bearing chloride, bromide, or acetate leaving groups, for example, resulted in the same shift from position 4a to 1,^[5] while direct substitutions are also known.^[5c] The generally proposed rationale for the shift occurring in these substitution reactions is an intermediate imine–

[a] Dr. N. Gulzar, Dr. K. M. Jones, Dr. M. Klussmann
Max-Planck-Institut für Kohlenforschung
Kaiser-Wilhelm-Platz 1, 45470 Mülheim an der Ruhr (Germany)
E-mail: klusi@mpi-muelheim.mpg.de

[b] H. Konnerth, Dr. M. Breugst
Universität zu Köln
Department für Chemie
Greinstraße 4, 50939 Köln (Germany)
E-mail: mbreugst@uni-koeln.de

Supporting information for this article is available on the WWW under <http://dx.doi.org/10.1002/chem.201405376>.

enamine tautomerization that activates position 1 (Scheme 1 b). However, detailed mechanistic studies are lacking.

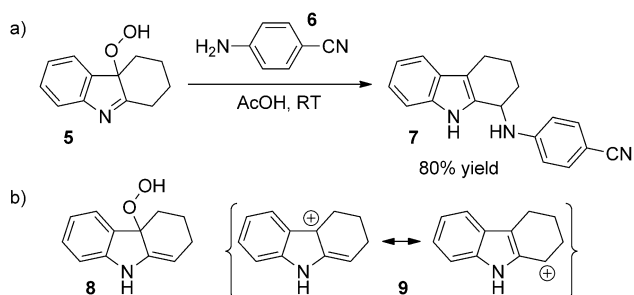
Another aspect of this reaction that is of interest to us is the utilization of a peroxide moiety as leaving group in acid-catalyzed reactions. Organic hydroperoxides can rearrange by O–O bond cleavage in the presence of acid, a well-known example is the key step in the industrial synthesis of phenol and acetone by the Hock process using cumyl hydroperoxide.^[6] On the other hand, acid-catalyzed nucleophilic substitution reactions of hydroperoxides by C–O bond cleavage are also known, albeit with a limited number of substrates.^[7] The reaction of singlet oxygen with indole derivatives is well-known to give rise to peroxides such as **2**.^[8] Methods that can utilize hydroperoxides selectively in substitution reactions would thus enable C–H functionalizations in two simple steps; by photocatalyzed aerobic oxygenation and subsequent acid-catalyzed substitution.

We have experienced that a detailed understanding of the reaction mechanism is extremely valuable in method development.^[7] Because we want to further extend the CHIPS concept into true one-pot C–H functionalization reactions, we started a detailed mechanistic investigation of the reaction shown in Scheme 1 a. Herein, the results of a combined experimental and computational study are presented.

Results and Discussion

Experimental studies

The reaction of choice for the mechanistic studies was the coupling of hydroperoxide **5** with *p*-cyanoaniline in acetic acid to give the substituted tetrahydrocarbazole **7** (Scheme 2 a). This reaction proceeds cleanly with high yields, which is also the case when the conditions are changed to methanol as solvent and trifluoroacetic acid as catalyst.^[3a]



Scheme 2. a) Model reaction for this mechanistic study; b) possible key intermediates **8** and **9** for S_N2' - and S_N1 -like pathways, respectively.

Possible scenarios for the acid-catalyzed substitution reaction, including the shift from position 4a to position 1, are attack of the aniline on the hydroperoxide **8** (and its protonated form, respectively) or the cation **9**, which can be viewed as S_N2' - and S_N1 -like mechanisms, respectively (Scheme 2 b). To distinguish between these two cases, kinetic studies appeared

most appropriate to determine the reaction order with respect to both substrates **5** and **6**.

We used ^1H NMR spectroscopy to determine formation of **7** from experiments that were quenched by base to stop the reaction at fixed intervals. Each reaction was repeated two to three times to ensure reproducibility. A polynomial curve of third order was fitted to the average conversion versus time profile, the first derivative of which then delivered the reaction rate profile (see the Supporting Information for further details).

To determine the reaction order in aniline **6**, a series of experiments with constant concentrations of peroxide **5** and varying concentrations of **6** was conducted, with **6** being in excess over **5**. The initial reaction rates were found to be slightly irregular but nearly constant at different concentrations of **6** (Figure 1).

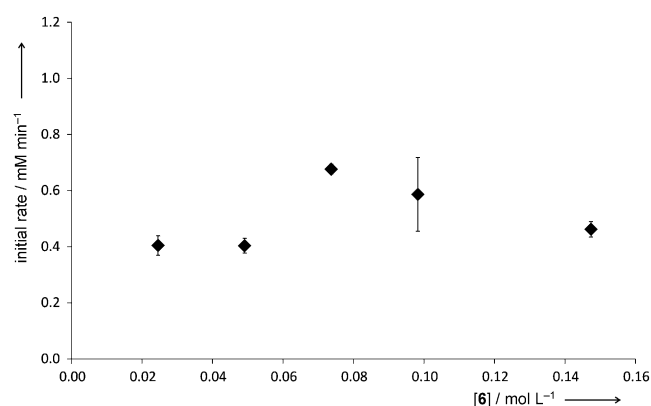


Figure 1. Determining the reaction order in aniline **6** for the reaction shown in Scheme 2 a, plotting initial rates versus $[\text{6}]_0$. All reactions: 0.05 M **5**, AcOH solvent, 26.5 °C.

As an approximation, the reaction order in **6** appears to be zero. The irregularity of the kinetic behavior could be due to the fact that the product precipitates during the reaction and that larger excesses of the weakly basic aniline nucleophiles reduce the final product yield, as was observed before.^[3a]

The reaction order in peroxide **5** was determined in the same way by varying its concentration while keeping all other parameters constant (Figure 2). For this set of experiments, the peroxide was used equimolar or in excess compared to the aniline.

The rate is clearly increasing with an increasing concentration of peroxide **5**, and from a linear regression analysis a reaction order in **5** of approximately 1.0 could be derived.

A graphical evaluation of this kinetic data, by using the reaction progress kinetic analysis method,^[9] leads to the same conclusions (see the Supporting Information). Similar results were also obtained from kinetic studies using reaction calorimetry for reactions with trifluoroacetic acid as catalyst in methanol and DMSO, respectively. These experiments revealed approximate reaction orders of 0.7 and 1.0, respectively, in **5**, zero in **6** and 1.0 in acid (see the Supporting Information). Although the rate behavior appears to be more complex, these findings clearly support an approximate rate expression for the reaction

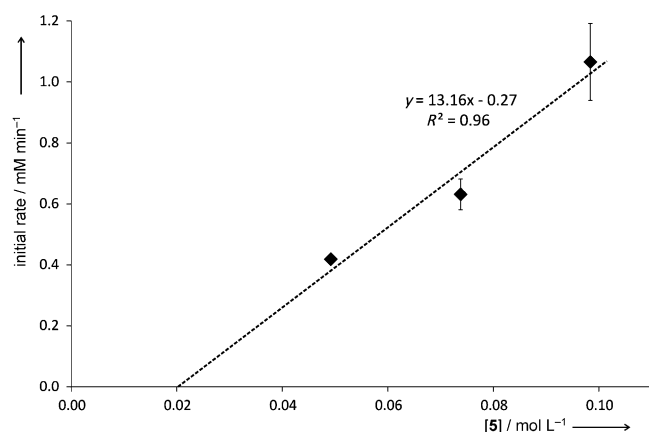
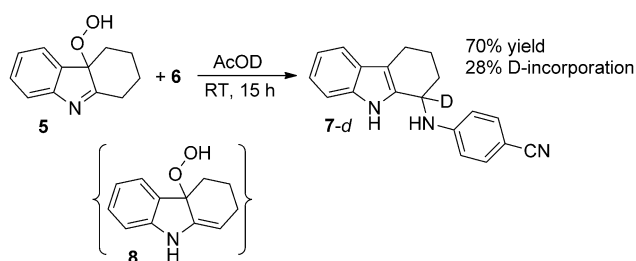


Figure 2. Determining the reaction order in peroxide **5** for the reaction shown in Scheme 2a; plotting initial rates versus $[5]_0$. All reactions: 0.05 M **6**, AcOH solvent, 26.5 °C.

in acetic acid as given in Equation (1) and accordingly an S_N1 -like mechanism via carbocation **9** (Scheme 2b).

$$r \approx k \cdot [5] \quad (1)$$

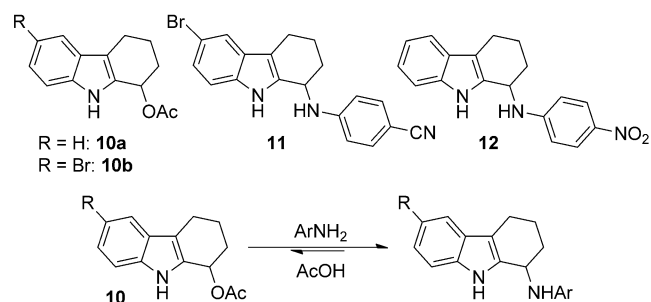
The next question of interest to us was how the postulated cationic intermediate **9** was formed. For this purpose, the reaction was performed in deuterated acetic acid. A deuterium incorporation of approximately 28% was detected at position 1 of the coupling product **7-d** (Scheme 3, see the Supporting Information for further details).



Scheme 3. Deuterium incorporation during the reaction in AcOD and postulated enamine tautomer **8**.

This partial incorporation of deuterium at position 1 suggests an acid-catalyzed equilibrium between imine **5** and its enamine tautomer **8** prior to formation of the cation **9**. Attempts to detect the enamine by NMR spectroscopy were unsuccessful. This and the relatively low incorporation of deuterium suggest that **8** is highly reactive and reacts to afford the coupling product before complete equilibrium H-D exchange is achieved.

During ^1H NMR analysis of the reaction mixture, we observed indications for the intermediacy of acetoxy-substituted tetrahydrocarbazole **10a**, but the product could not be isolated for characterization. We could, however, isolate the corresponding acetate **10b** from 6-bromo tetrahydrocarbazole and confirm its



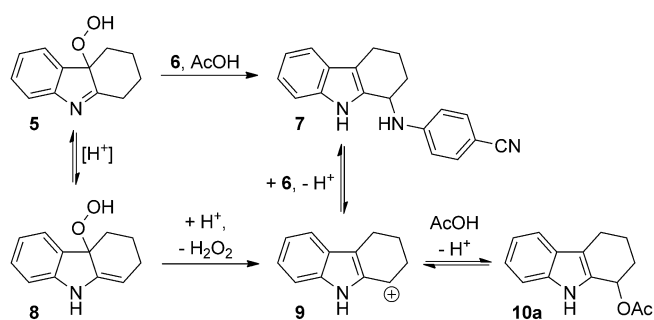
Scheme 4. Reversible formation of substitution products with solvent and anilines.

structure (Scheme 4). When subjected to reaction conditions, most of **10b** converted to **11**, and when **11** was dissolved in acetic acid, it partially converted to **10b**. Likewise, we found that the coupling product with *p*-nitroaniline, **12**, could be partially converted to **7** when treated with **6**, and vice versa. A competition experiment of **5** with both anilines gave a mixture of products **7** and **12** in a 1:1 ratio. All of these results suggest that the postulated intermediate cation **9** can be trapped by solvent and aniline nucleophiles alike, that all of these products are formed reversibly and that the trapping products with anilines are thermodynamically favored (Scheme 4; see the Supporting Information for details).

To detect H_2O_2 , which would be liberated according to the proposed mechanism of Scheme 2b, we analyzed a reaction mixture after two hours, at which point full conversion of the peroxide had been attained. On adding an acidic solution of $\text{K}_2\text{Cr}_2\text{O}_7$, the mixture turned blue, indicating the formation of $\text{CrO}(\text{O}_2)_2$.^[10] We had shown previously that this method had a negligible cross sensitivity with an organic hydroperoxide,^[7] which was also confirmed for **5**.

Based on all of the above-mentioned observations, we conclude that the acid-catalyzed tautomerization of imine **5** to enamine **8** is followed by C–O bond cleavage to give resonance-stabilized carbocation **9** and hydrogen peroxide. The added nucleophile **6** or the solvent can trap **9** to form the coupling product **7** and the less-stable adduct **10a**, both of which exist in equilibrium with **9** (Scheme 5).

All attempts to observe **8** or **9** by studying the reaction of **5** in the presence of acid separately only led to decomposition

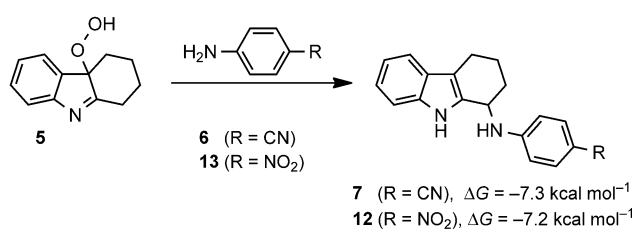


Scheme 5. Proposed reaction mechanism, based on experimental studies.

into mostly unidentified byproducts. As the kinetic experiments were also not entirely conclusive and the negative reaction order in **6** potentially indicates a more complex mechanism, we looked for additional insight from computational studies.

Computational studies

As the computational approach also allows the study of intermediates that are too unstable to be observed experimentally, we analyzed the putative reaction mechanisms employing density functional theory [M06-2X-D3/def2-TZVPP/IEFPCM//M06-2X-D3/6-1+G(d,p)/IEFPCM(MeOH)]. Although most experiments presented herein were performed in acetic acid as solvent, it has been shown previously that similar results are obtained in methanolic solution with trifluoroacetic acid as Brønsted acid.^[3a] Since calculations using methanol and acetic acid as solvents gave very similar results, we chose to use methanol as the solvent and trifluoroacetic acid as Brønsted acid for the computational studies. In methanol, direct solvent participation especially in proton-transfer reactions, is somewhat less likely due to the lower acidity. Furthermore, the computational investigations employed 4-nitroaniline (**13**) instead of the cyanoaniline **6**. Previous studies have already shown that both nucleophiles are similarly reactive and should react through the same reaction mechanism.^[3a] Further validation for comparable reactivities comes from almost equal reaction free energies for the combinations of differently substituted anilines (e.g., **6** or **13**) and tetrahydrocarbazole peroxide **5** (Scheme 6; see the Supporting Information for more details). The computational result of comparable stabilities of **7** and **12** agrees nicely with the results from the competition experiment between **6** and **13**.



Scheme 6. Overall thermodynamics for the reactions of the differently substituted anilines **6** and **13** and tetrahydrocarbazole peroxides (**5**) [in kcal mol⁻¹, M06-2X-D3/def2-TZVPP/IEFPCM//M06-2X-D3/6-31+G(d,p)/IEFPCM(MeOH)].

Prior to the analysis of the complete reaction mechanism, we investigated whether the initially formed tetrahydrocarbazole peroxide could undergo isomerization reactions. The experimental studies suggested that peroxide **5** tautomerizes to the enamine isomer **8** (see above). Additional isomerizations (\rightarrow **14**, **15**; Figure 3) could also occur via acid-catalyzed dissociation–association reactions or through [3,3]-sigmatropic rearrangements of the protonated peroxides. Figure 3 summarizes the relative thermodynamic stabilities ($\Delta\Delta G$) of the most

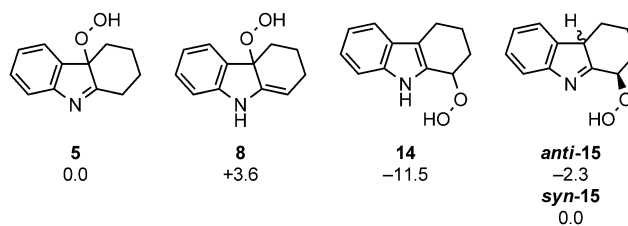
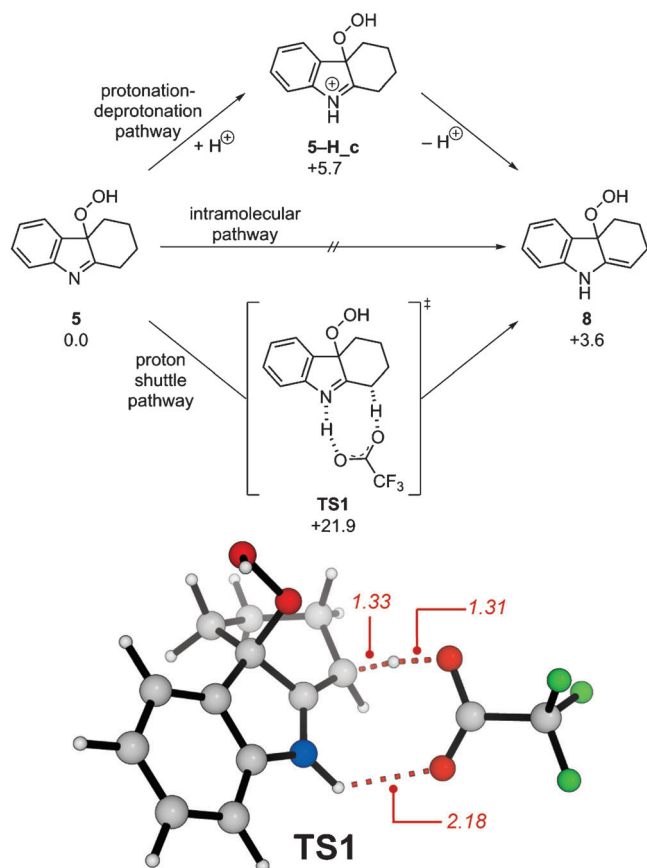


Figure 3. Putative isomeric tetrahydrocarbazole peroxides and their relative stabilities [in kcal mol⁻¹, M06-2X-D3/def2-TZVPP/IEFPCM//M06-2X-D3/6-31+G(d,p)/IEFPCM(MeOH)].

stable conformers. The peroxide **5**, isolated from the photooxygenation reaction, with an imine substructure is more stable than the isomer with an enamine substructure **8**, which can be rationalized by the stabilization of the annulated benzene ring. Aromaticity within the indole is restored in **14**, which renders **14** the most stable peroxide ($\Delta\Delta G = -11.5 \text{ kcal mol}^{-1}$). The corresponding imines *anti*-**15** and *syn*-**15** were calculated to be slightly more stable or isoenergetic compared to the initially formed peroxide **5**. As neither **14**, *anti*-**15** nor *syn*-**15** could be observed under the experimental conditions, we have to conclude that their formation is kinetically hindered or that they are rapidly consumed under the reaction conditions. As treatment of **5** with acid in the absence of any nucleophiles does not result in clean formation of **14** or **15** but in decomposition to a mixture of mostly unknown products, the former explanation is more likely.

As the tautomerization of **5** to **8** could be an important step along the reaction mechanism, we had a closer look at this isomerization. In principle, three different pathways have to be considered for this isomerization; a direct, intramolecular proton transfer, protonation and deprotonation, or a trifluoroacetic acid-catalyzed proton shuttle (Scheme 7). Intramolecular processes can be ruled out as previous investigations revealed barriers of $>60 \text{ kcal mol}^{-1}$ for these transformations.^[11] According to our calculations, the initial N-protonation of **5** yielding **5-H_c** occurs readily without a significant barrier, but we were unable to locate any transition states for a deprotonation at the carbon terminus (\rightarrow **8**). Instead, all estimated transition states converged to the structure for a proton shuttle transition state **TS1** ($\Delta G^\ddagger = 21.9 \text{ kcal mol}^{-1}$). Protonation at the nitrogen atom is almost complete and the deprotonation of the carbon atom lacks behind, which renders **TS1** highly asynchronous. The intrinsic reaction coordinate (IRC) starting from **TS1** confirmed that **5** is transformed to **8** via this transition state. Based on these results, we conclude that a proton shuttle mechanism via trifluoroacetic acid is most likely for the tautomerization of **5** to **8**. The high barrier and the endergonic formation of **8** are in line with the failure to detect **8** by ¹H NMR spectroscopy, but its presence was supported indirectly by the reaction in AcOD (Scheme 3).

In the first step of the proposed mechanism, protonation of tetrahydrocarbazole peroxide takes place. Therefore, we analyzed the stabilities of all possible protonated species (i.e., protonation at O1, O2, and the nitrogen atoms). As we cannot rule out the participation of the peroxides **14** and **15** based on



Scheme 7. Different mechanisms for the tautomerization of the imine **5** to the enamine **8** catalyzed by trifluoroacetic acid [in kcal mol⁻¹, M06-2X-D3/def2-TZVPP/IEFPCM//M06-2X-D3/6-31 + G(d,p)/IEFPCM(MeOH)].

experimental studies alone, we decided to keep them for the computational analysis for the sake of completeness. These results are summarized in Figure 4.

In general, the nitrogen atom is the most basic center of the tetrahydrocarbazole system and consequently, protonation at this atom leads to the most stable cationic structures. These *N*-protonated peroxides do not lie on the reaction coordinate for the transformation under investigation, and protonation at the oxygen atom is needed for the reaction to proceed. However, protonation of either oxygen is significantly higher in energy ($\Delta\Delta G > 14.3$ kcal mol⁻¹). As a result, the concentration of *O*-protonated peroxides in solution should be rather small. Interestingly, no stable protonated adduct **8-H_a** could be located on the potential energy surface. Protonation of the oxygen atom of peroxide **8** resulted in an immediate C–O bond fission with formation of a stabilized carbocation (\rightarrow **9**) and hydrogen peroxide.

Subsequently, hydrogen peroxide is released from the protonated species and a carbocation is formed. Different possibilities have been evaluated and are summarized in Scheme 8, and the different transition states are depicted in Figure 5. Three different allyl cations (**9**, **16a** and **16b**) could be formed from the corresponding protonated peroxides. Our calculations indicate that the aza-allyl cations **16a** and **16b** are significantly higher in energy than the analogue **9** ($\Delta\Delta G = 37.6$ and

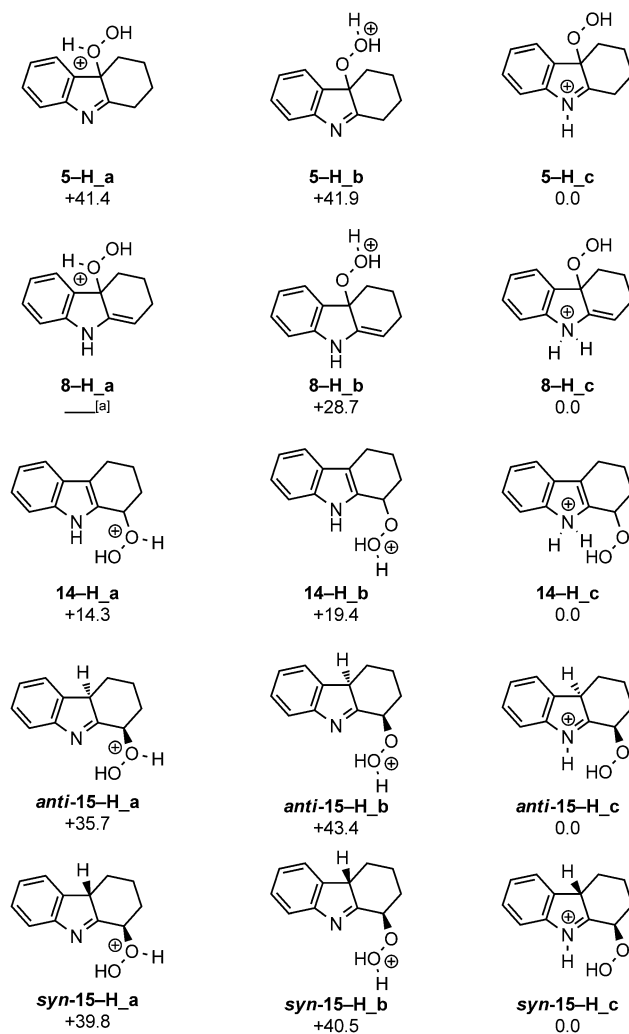


Figure 4. Relative stabilities of differently protonated tetrahydrocarbazole peroxides [in kcal mol⁻¹, M06-2X-D3/def2-TZVPP/IEFPCM//M06-2X-D3/6-31 + G(d,p)/IEFPCM(MeOH)]; [a] could not be located, see main text.

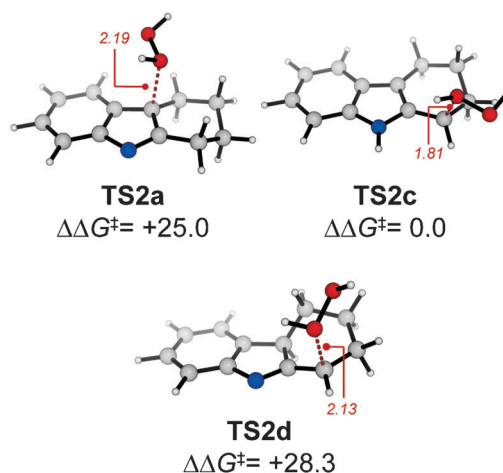
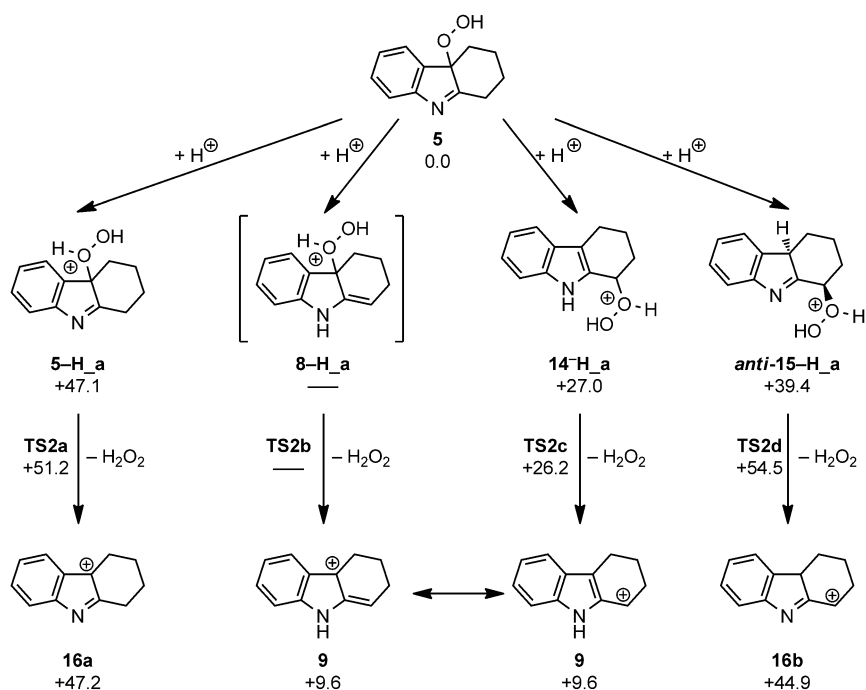


Figure 5. Transition states for the dissociation of hydrogen peroxide, relative activation free energies (in kcal mol⁻¹) and selected bond lengths (in Å) [M06-2X-D3/def2-TZVPP/IEFPCM//M06-2X-D3/6-31 + G(d,p)/IEFPCM(MeOH)].

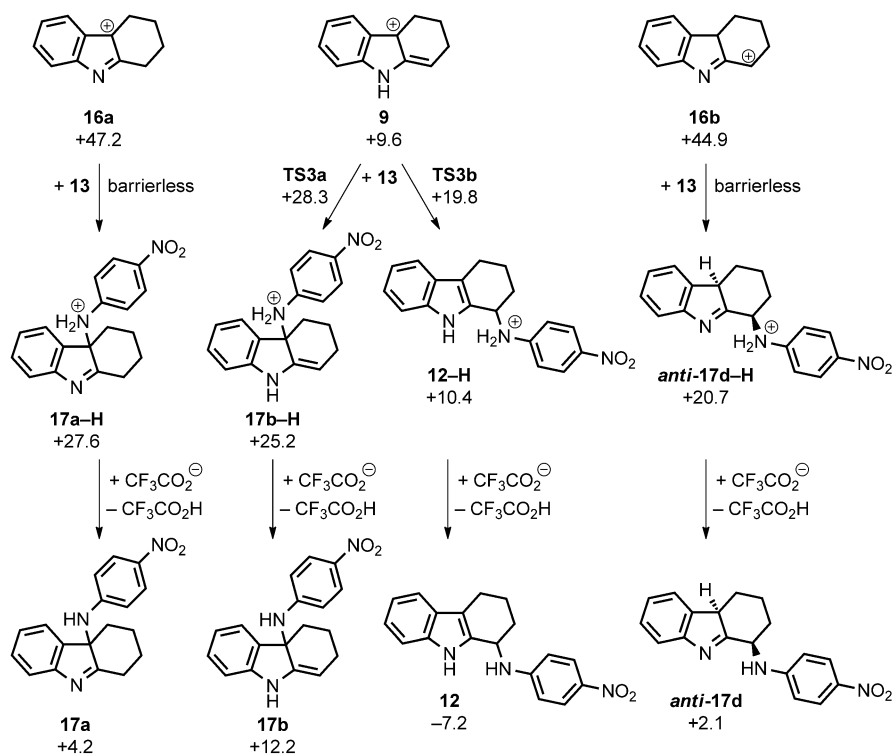


Scheme 8. Different pathways for hydrogen peroxide dissociation from protonated tetrahydrocarbazole peroxides with respect to the initially generated peroxide **5** [in kcal mol⁻¹, M06-2X-D3/def2-TZVPP/IEFPCM//M06-2X-D3/6-31 + G(d,p)/IEFPCM(MeOH)].

35.3 kcal mol⁻¹, respectively). Whereas a protonation of the oxygen atom of the enamine tautomer **8** directly leads to the carbocation **9** in a concerted fashion without the formation of the protonated peroxide **8-H_a**, transition states could be located for hydrogen peroxide cleavage in the other isomers. A very small barrier of 0.3 kcal mol⁻¹ between **14-H_a** and **TS2c** has been calculated on the M06-2X-D3/6-31 + G(d,p)/IEFPCM potential energy surface, whereas negative barriers were obtained from high-level M06-2X single-point calculations. Thus, the conversion of **14-H_a** to **9** via **TS2c** occurs without a significant barrier. While **9** can be formed easily, transition states for the formation of the aza-allyl cations **16a** and **16b** are considerably higher ($\Delta G^\ddagger = 51.2$ and 54.5 kcal mol⁻¹, respectively; Scheme 8 and Figure 5). The breaking C–O bond is significantly longer in **TS2a** and **TS2d** than in **TS2c** reflecting the highly exergonic reaction from **14-H_a** to **9** ($\Delta\Delta G = -17.4$ kcal mol⁻¹) and

therefore a much earlier transition state. The high energies of both intermediates and transition states render the formation of **16a** or **16b** very unlikely.

In principle, each cationic intermediate could now be attacked by a nucleophile (Scheme 9). The unstable aza-allyl cations **16a** and **16b** (if formed at all) are so reactive that they will undergo combinations with *p*-nitroaniline (**13**) without significant barriers (\rightarrow **17a-H** or *anti*-**17d-H**). In contrast, transition states could be obtained for the nucleophilic attack of **13** on both ends of the less reactive isomer **9**. The attack at the indole substructure through **TS3a** yields the ammonium ion **17b-H** in an endergonic reaction. The attack at the cyclohexane substructure results not only in the most stable ammonium ion **12-H** but also proceeds through the more favorable transition state **TS3b** (Scheme 9, Figure 6). In both transition states, stabilizing π - π interactions between the aromatic



Scheme 9. Different pathways for the nucleophilic attack of 4-nitroaniline (**13**) on the allyl cations **14** [free energies in kcal mol⁻¹ with respect to **05**, M06-2X-D3/def2-TZVPP/IEFPCM//M06-2X-D3/6-31 + G(d,p)/IEFPCM(MeOH)].

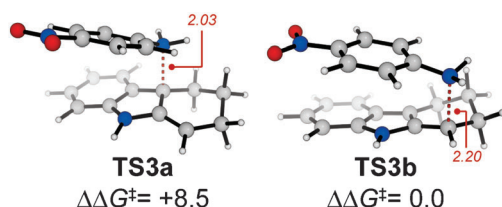
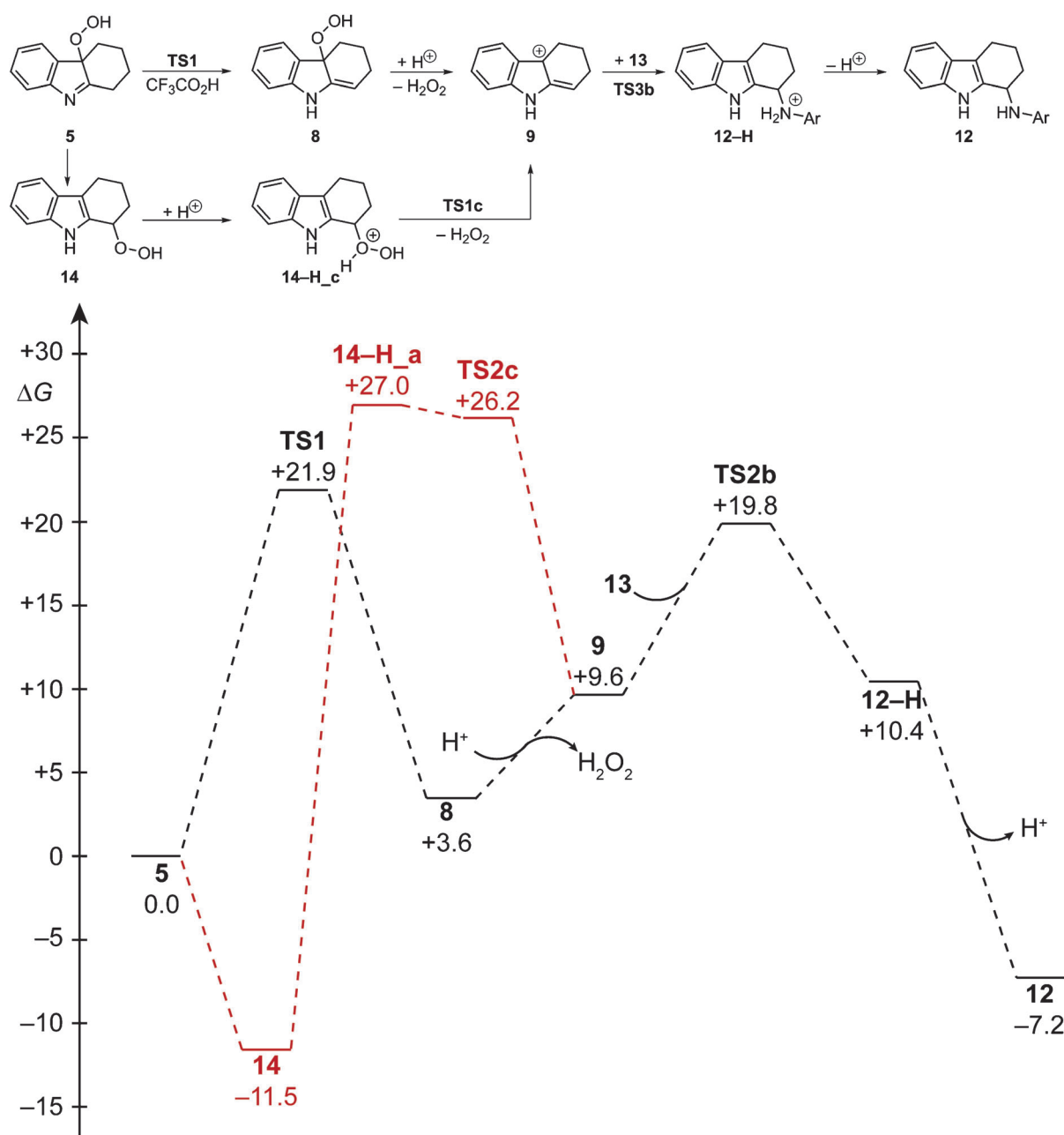


Figure 6. Transition states for the nucleophilic attack of **13** on the allyl cation **9**, relative activation free energies (in kcal mol⁻¹) and selected bond lengths (in Å) [M06-2X-D3/def2-TZVPP/IEFPCM//M06-2X-D3/6-31+G(d,p)/IEFPCM(MeOH)].

rings render the aryl groups almost parallel. The shorter C–N bond length in **TS3a** (Figure 6) can again be rationalized with the endergonicity of this step and thereby with a later transition state. Attempts to locate the analogous S_N2 or S_N2' transition states (Scheme 2b) starting from different transition state guesses failed, which further supports the experimental evidence for an S_N1-type mechanism.

Deprotonation of the ammonium ions affords the final substitution products **12** and **17**. Among those, the experimentally isolated isomer **12** is by far the most stable (Scheme 9). As **12** is the only isomer in which the indole substructure has been reinstalled, it is not surprising that **12** is the only product that is formed in an overall exergonic reaction.

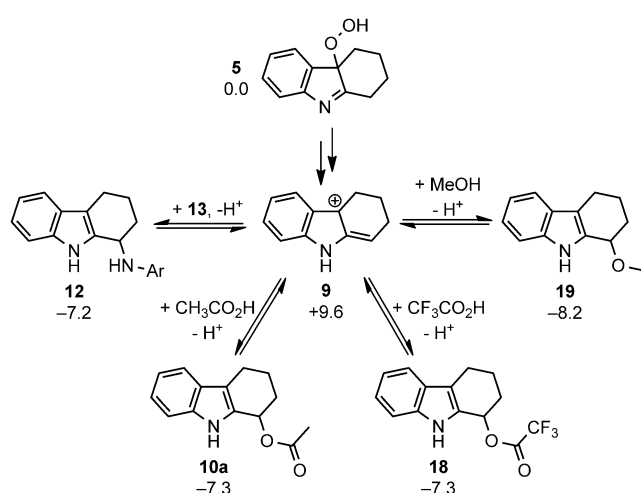


Scheme 10. Calculated Gibbs free energy profiles for the formation of the substitution product **12** from the peroxide **5** and the aniline **13** [in kcal mol⁻¹, M06-2X-D3/def2-TZVPP/IEFPCM//M06-2X-D3/6-31+G(d,p)/IEFPCM(MeOH)].

Based on the computational analysis presented above, two pathways are conceivable for the C–H functionalization and the corresponding Gibbs free energy profiles are shown in Scheme 10. The lowest energy pathway (black lines in Scheme 10) involves the initial tautomerization to the enamine isomer **8**, protonation and elimination of hydrogen peroxide and subsequent nucleophilic attack of aniline. The rate-limiting step for this pathway was calculated to be the initial isomerization (**TS1**), which is in line with the experimentally determined rate law (first order in peroxide, zeroth order in aniline, first order in acid if used in catalytic amounts in DMSO or methanol). The calculated activation free energy of $21.9 \text{ kcal mol}^{-1}$ is in good qualitative agreement with the experimental reaction times of two to four hours. As an alternative, the initially generated peroxide **5** could isomerize to the thermodynamically most stable peroxide **14**. In this case, the dissociation of hydrogen peroxide would be the rate-limiting step. However, as this would require an activation free energy of more than 38 kcal mol^{-1} and there is no experimental evidence for an involvement of **14**, this pathway has to be discarded.

As mentioned above, the cationic intermediate **9** can be reversibly trapped by various nucleophiles and we have additionally calculated the stabilities of these intermediates (Scheme 11). All products are formed in exergonic reactions and all reaction free energies fall in a very small energy range of only 1 kcal mol^{-1} . When free energies are considered, only the methanol adduct **19** was calculated to be slightly more favorable than the amino product **12**. However, **12** is slightly preferred ($\Delta\Delta H = 1.1 \text{ kcal mol}^{-1}$) when reaction enthalpies are compared, which is in line with the experimental preference of **12** over **19**. Additionally, product **12** precipitates during the reaction, further driving the equilibrium to its side.

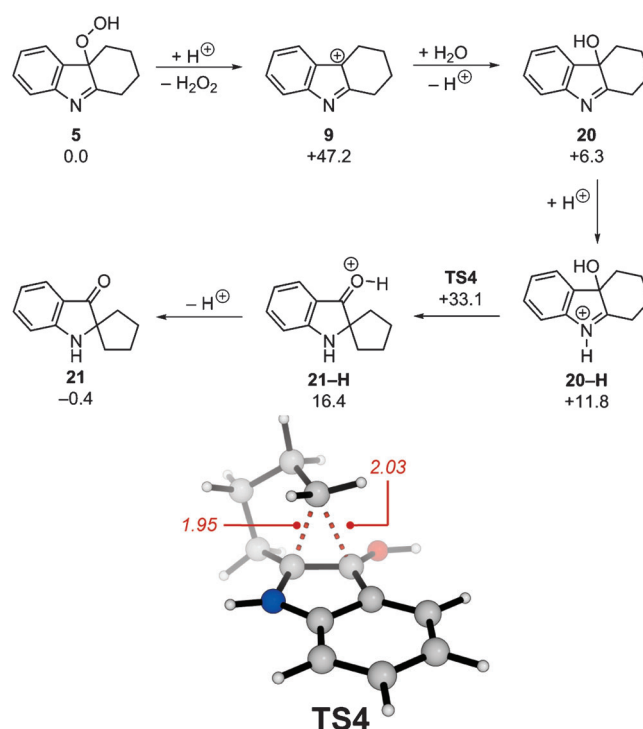
The reversible formation of **12** also explains the diastereoselectivities we had previously observed in products bearing a substituent in the annulated cyclohexane ring.^[3a] The major



Scheme 11. Thermodynamic stabilities of different products obtained from nucleophilic attack on the intermediate carbocation **9** [free energies in kcal mol^{-1} M06-2X-D3/def2-TZVPP/IEFPCM//M06-2X-D3/6-31 + G(d,p)/IEFPCM(MeOH)].

diastereomer isolated in the experimental studies is preferred both thermodynamically and kinetically (see the Supporting Information for a detailed discussion).

Especially in reactions with low conversion to the desired products, we could observe and characterize the spirocyclic indolinone by-product **21**. This could be formed from the tetrahydrocarbazole alcohol **20**, which in turn might be generated either by reduction of the corresponding peroxide **5** or by the attack of water on the allyl cation **9** (Scheme 12). The former is probably more likely, as the formation of **16a** is highly endergonic. The alcohol **20** is subsequently protonated at the nitrogen atom and the resulting β -hydroxy iminium ion **20–H** undergoes a ring contraction through **TS3**. This step requires a substantial activation free energy ($\Delta G^\ddagger = 33.1 \text{ kcal mol}^{-1}$). The cationic ketone **21–H** is subsequently deprotonated to yield the spiro compound **21** in an overall almost thermoneutral reaction. The rate-limiting step for this reaction is significantly higher than those for the formation of the amino product **12** (see above) and therefore, the spiro compound will not be formed in significant amount.



Scheme 12. Formation of a spiro-indolinone **21** and the rate-limiting transition state **TS4** as a potential side reaction [in kcal mol^{-1} , M06-2X-D3/def2-TZVPP/IEFPCM//M06-2X-D3/6-31 + G(d,p)/IEFPCM(MeOH)].

Conclusions

In summary, our combined experimental and computational investigations of the reaction of hydroperoxide **5** with aniline **6** in acetic acid support an acid-mediated nucleophilic substitution of hydrogen peroxide via an S_N1 -like mechanism. The observed shift of the leaving group at position 4a to the new C–N bond at position 1 is rationalized by an acid-mediated tauto-

merization of the imine form of the hydroperoxide to an enamine, which generates a stabilized allylic cation after loss of hydrogen peroxide. Computational investigations indicate that the rate-limiting step is this initial tautomerization, which is in excellent agreement with the reaction orders from kinetic studies and the incorporation of deuterium during the reaction in deuterated acetic acid. These investigations could be relevant for other reactions with tetrahydrocarbazole derivatives bearing a leaving group at position 4a. They also support the strategy of C–H functionalization via intermediate peroxides (CHIPS) and could be helpful in future extensions towards other substrates.

Experimental Section

Experimental Details

Unless otherwise indicated, all reagents and solvents were purchased from commercial distributors and used as received. The hydroperoxide **5** and the products **7** and **12** were prepared according to published procedures.^[3a,8e] For ¹H and ¹³C NMR spectra of new compounds and further details of kinetic and other experiments, see the Supporting Information.

Computational Details

For all intermediates of the C–H functionalization of tetrahydrocarbazole, the conformational space was explored using the OPLS-2005 force field^[12] and a modified Monte Carlo search routine implemented in MacroModel version 9.8.^[13] An energy cut-off of 20 kcal mol⁻¹ was used for the conformational analysis, and structures with heavy-atom RMSDs less than 1 Å after the initial force field optimization were considered to be the same conformer. The remaining structures were subsequently optimized with the *meta*-hybrid M06–2X functional,^[14] Grimme's D3 dispersion correction (zero-damping),^[15] and the double- ζ basis set 6-31+G(d,p). Solvation by methanol was accounted for by using the integral equation formalism polarizable continuum model (IEFPCM) for all calculations (optimizations, frequencies, and single-point energies).^[16] Polarizable continuum models do not have a large impact on the calculated frequencies, but might be necessary for the location of transition states in some cases.^[17] Vibrational analysis verified that each structure was a minimum or a transition state. Following the intrinsic reaction coordinates (IRC) confirmed that all transition states connected the corresponding reactants and products on the potential energy surface. Thermal corrections were calculated from unscaled harmonic vibrational frequencies at the same level of theory for a standard state of 1 mol L⁻¹ and 298.15 K. Entropic contributions to the reported free energies were calculated from partition functions evaluated with Truhlar's quasiharmonic approximation.^[17] This method uses the same approximations as the usual harmonic oscillator approximation except that all vibrational frequencies lower than 100 cm⁻¹ are set equal to 100 cm⁻¹ to correct for the breakdown of the harmonic oscillator approximation for low frequencies. Electronic energies were subsequently obtained from single-point calculations employing the M06-2X functional with the large triple- ζ def2-TZVPP basis set,^[18] IEFPCM for methanol, and Grimme's D3 dispersion correction. An ultrafine grid corresponding to 99 radial shells and 590 angular points was used throughout this investigation for numerical integration of the density.^[19] The reported free energies refer to the lowest-energy conformer and are almost identical to those obtained from Boltz-

mann-averaged ensembles. All DFT calculations were performed with Gaussian 09.^[20]

Acknowledgements

Financial support from the DFG (KL 2221/3-1 and Heisenberg scholarship to M.K., KL 2221/4-1), the Fonds der chemischen Industrie (Liebig scholarship to M.B.) and the MPI für Kohlenforschung is gratefully acknowledged. We thank Philipp Schulze for support with the analysis of H₂O₂. This work used the Cologne High Efficiency Operating Platform for Sciences (CHEOPS).

Keywords: computational chemistry · kinetics · nitrogen heterocycles · peroxides · reaction mechanisms

- [1] a) N. Gulzar, B. Schweitzer-Chaput, M. Klussmann, *Catal. Sci. Technol.* **2014**, *4*, 2778–2796; b) S. A. Girard, T. Knauber, C.-J. Li, *Angew. Chem.* **2014**, *126*, 76–103; *Angew. Chem. Int. Ed.* **2014**, *53*, 74–100; c) C. Zheng, S.-L. You, *RSC Adv.* **2014**, *4*, 6173–6214; d) R. Rohlmann, O. G. Mancheño, *Synlett* **2013**, *24*, 6–10; e) C. S. Yeung, V. M. Dong, *Chem. Rev.* **2011**, *111*, 1215–1292; f) C. Liu, H. Zhang, W. Shi, A. Lei, *Chem. Rev.* **2011**, *111*, 1780–1824; g) M. Klussmann, D. Sureshkumar, *Synthesis* **2011**, 353–369; h) C. J. Scheuermann, *Chem. Asian J.* **2010**, *5*, 436–451; i) A. R. Dick, M. S. Sanford, *Tetrahedron* **2006**, *62*, 2439–2463.
- [2] a) Z. Shi, C. Zhang, C. Tang, N. Jiao, *Chem. Soc. Rev.* **2012**, *41*, 3381–3430; b) A. N. Campbell, S. S. Stahl, *Acc. Chem. Res.* **2012**, *45*, 851–863.
- [3] a) N. Gulzar, M. Klussmann, *Org. Biomol. Chem.* **2013**, *11*, 4516–4520; b) N. Gulzar, M. Klussmann, *J. Visualized Exp.* **2014**, *88*, e51504 (DOI: 51510.53791/51504).
- [4] a) S. D. Boggs, K. S. Gudmundsson, L. D. A. Richardson, P. R. Sebahar, *Tetrahydrocarbazole derivatives and their pharmaceutical use*, WO 2004/110999A1, **2004**; b) K. S. Gudmundsson, *HCV Inhibitors*, WO 2006/121467A2, **2006**.
- [5] a) F. Ying-Hsiueh Chen, E. Leete, *Tetrahedron Lett.* **1963**, *4*, 2013–2017; b) R. J. Owellen, *J. Org. Chem.* **1974**, *39*, 69–72; c) R. J. Owellen, C. A. Hartke, *J. Org. Chem.* **1976**, *41*, 102–104; d) C. Chan, C. Li, F. Zhang, S. J. Danishefsky, *Tetrahedron Lett.* **2006**, *47*, 4839–4841; e) K. Higuchi, M. Tayu, T. Kawasaki, *Chem. Commun.* **2011**, 47, 6728–6730; f) R. E. Ziegler, S.-J. Tan, T.-S. Kam, J. A. Porco, *Angew. Chem.* **2012**, *124*, 9482–9485; *Angew. Chem. Int. Ed.* **2012**, *51*, 9348–9351; g) H. Zaimoku, T. Hatta, T. Taniguchi, H. Ishibashi, *Org. Lett.* **2012**, *14*, 6088–6091.
- [6] a) H. Hock, S. Lang, *Ber. Dtsch. Chem. Ges.* **1944**, *77*, 257–264; b) H. Hock, H. Kropf, *Angew. Chem.* **1957**, *69*, 313–321.
- [7] See for example: a) A. G. Davies, R. V. Foster, R. Nery, *J. Chem. Soc.* **1954**, 2204–2209; b) C. W. Jefford, J. C. Rossier, S. Kohmoto, J. Boukouvalas, *Helv. Chim. Acta* **1985**, *68*, 1804–1814; c) I. Saito, H. Nakagawa, Y. H. Kuo, K. Obata, T. Matsuura, *J. Am. Chem. Soc.* **1985**, *107*, 5279–5280; d) L. Liguori, H.-R. Bjorsvik, F. Fontana, D. Bosco, L. Galimberti, F. Minisci, *J. Org. Chem.* **1999**, *64*, 8812–8815; e) P. H. Dussault, H.-J. Lee, X. Liu, *J. Chem. Soc. Perkin Trans. 1* **2000**, 3006–3013; f) Á. Pintér, A. Sud, D. Sureshkumar, M. Klussmann, *Angew. Chem.* **2010**, *122*, 5124–5128; *Angew. Chem. Int. Ed.* **2010**, *49*, 5004–5007; g) Á. Pintér, M. Klussmann, *Adv. Synth. Catal.* **2012**, *354*, 701–711; h) C. G. Piscopo, S. Buhler, G. Sartori, R. Maggi, *Catal. Sci. Technol.* **2012**, *2*, 2449–2452; i) B. Schweitzer-Chaput, A. Sud, Á. Pinter, S. Dehn, P. Schulze, M. Klussmann, *Angew. Chem.* **2013**, *125*, 13470–13474; *Angew. Chem. Int. Ed.* **2013**, *52*, 13228–13232.
- [8] For reviews, see: a) M. V. George, V. Bhat, *Chem. Rev.* **1979**, *79*, 447–478; b) M. R. Ilesce, F. Cermola, F. Temussi, *Curr. Org. Chem.* **2005**, *9*, 109–139; for tetrahydrocarbazole, see: c) R. J. S. Beer, L. McGrath, A. Robertson, *J. Chem. Soc.* **1950**, 2118–2126; d) B. Witkop, J. B. Patrick, M. Rosenblum, *J. Am. Chem. Soc.* **1951**, *73*, 2641–2647; e) C. A. Mateo, A. Urrutia, J. G. Rodríguez, I. Fonseca, F. H. Cano, *J. Org. Chem.* **1996**, *61*, 810–812.

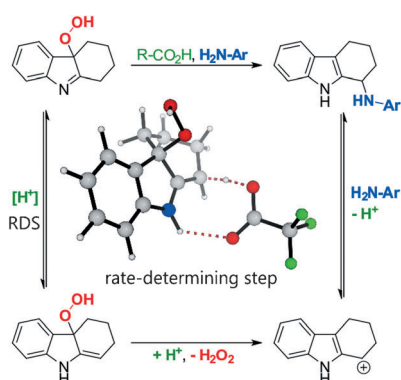
- [9] a) D. G. Blackmond, *Angew. Chem.* **2005**, *117*, 4374–4393; *Angew. Chem. Int. Ed.* **2005**, *44*, 4302–4320; b) J. S. Mathew, M. Klussmann, H. Iwamura, F. Valera, A. Futran, E. A. C. Emanuelsson, D. G. Blackmond, *J. Org. Chem.* **2006**, *71*, 4711–4722.
- [10] D. F. Evans, *J. Chem. Soc.* **1957**, *0*, 4013–4018.
- [11] a) J.-F. Lin, C.-C. Wu, M.-H. Lien, *J. Phys. Chem.* **1995**, *99*, 16903–16908; b) C.-C. Wu, M.-H. Lien, *J. Phys. Chem.* **1996**, *100*, 594–600; c) J. Andrés, L. R. Domingo, M. T. Picher, V. S. Safont, *Int. J. Quantum Chem.* **1998**, *66*, 9–24.
- [12] J. L. Banks, H. S. Beard, Y. Cao, A. E. Cho, W. Damm, R. Farid, A. K. Felts, T. A. Halgren, D. T. Mainz, J. R. Maple, R. Murphy, D. M. Philipp, M. P. Repasky, L. Y. Zhang, B. J. Berne, R. A. Friesner, E. Gallicchio, R. M. Levy, *J. Comput. Chem.* **2005**, *26*, 1752–1780.
- [13] MacroModel, V. 10.2, Schrödinger, LLC, New York, NY, **2013**.
- [14] Y. Zhao, D. G. Truhlar, *Theor. Chem. Acc.* **2008**, *120*, 215–241.
- [15] S. Grimme, J. Antony, S. Ehrlich, H. Krieg, *J. Chem. Phys.* **2010**, *132*, 154104.
- [16] E. Cancès, B. Mennucci, J. Tomasi, *J. Chem. Phys.* **1997**, *107*, 3032–3041.
- [17] R. F. Ribeiro, A. V. Marenich, C. J. Cramer, D. G. Truhlar, *J. Phys. Chem. B* **2011**, *115*, 14556–14562.
- [18] F. Weigend, R. Ahlrichs, *Phys. Chem. Chem. Phys.* **2005**, *7*, 3297–3305.
- [19] S. E. Wheeler, K. N. Houk, *J. Chem. Theory Comput.* **2010**, *6*, 395–404.
- [20] M. J. Frisch, G. W. Trucks, H. B. Schlegel, G. E. Scuseria, M. A. Robb, J. R. Cheeseman, G. Scalmani, V. Barone, B. Mennucci, G. A. Petersson, H. Nakatsuji, M. Caricato, X. Li, H. P. Hratchian, A. F. Izmaylov, J. Bloino, G. Zheng, J. L. Sonnenberg, M. Hada, M. Ehara, K. Toyota, R. Fukuda, J. Hasegawa, M. Ishida, T. Nakajima, Y. Honda, O. Kitao, H. Nakai, T. Vreven, J. A. Montgomery, Jr., J. E. Peralta, F. Ogliaro, M. Bearpark, J. J. Heyd, E. Brothers, K. N. Kudin, V. N. Staroverov, R. Kobayashi, J. Normand, K. Raghavachari, A. Rendell, J. C. Burant, S. S. Iyengar, J. Tomasi, M. Cossi, N. Rega, J. M. Millam, M. Klene, J. E. Knox, J. B. Cross, V. Bakken, C. Adamo, J. Jaramillo, R. Gomperts, R. E. Stratmann, O. Yazyev, A. J. Austin, R. Cammi, C. Pomelli, J. W. Ochterski, R. L. Martin, K. Morokuma, V. G. Zakrzewski, G. A. Voth, P. Salvador, J. J. Dannenberg, S. Dapprich, A. D. Daniels, Ö. Farkas, J. B. Foresman, J. V. Ortiz, J. Cioslowski, D. J. Fox, Gaussian 09, revision D.01; Gaussian, Inc., Wallingford CT, **2009**.

Received: September 23, 2014

Published online on ■ ■ ■ ■, 0000

FULL PAPER

Substitute a hydroperoxide: Tetrahydrocarbazoles can undergo a C–H amination via intermediate hydroperoxides and acid-catalyzed substitution with anilines. The mechanism of this reaction was studied by kinetics and DFT calculations and an initial imine–enamine tautomerization was found to be the rate-determining step.



Reaction Mechanisms

N. Gulzar, K. M. Jones, H. Konnerth,
M. Breugst,* M. Klussmann*



Experimental and Computational
Studies on the C–H Amination
Mechanism of Tetrahydrocarbazoles
via Hydroperoxides

